Supporting Information

CO_2 Electroreduction Performance of PtS_2 Supported Single Transition Metal Atoms: A Theoretical Study

Yu-wang Sun, Jing-yao Liu*

Institute of Theoretical Chemistry, College of Chemistry, Jilin University, Changchun 130023, People's Republic of China

Submitted to: ***Phys. Chem. Chem. Phys.***

*Corresponding author: Dr. Jing-yao Liu;
E-mail address: ljy121@jlu.edu.cn. (J.Y. Liu)

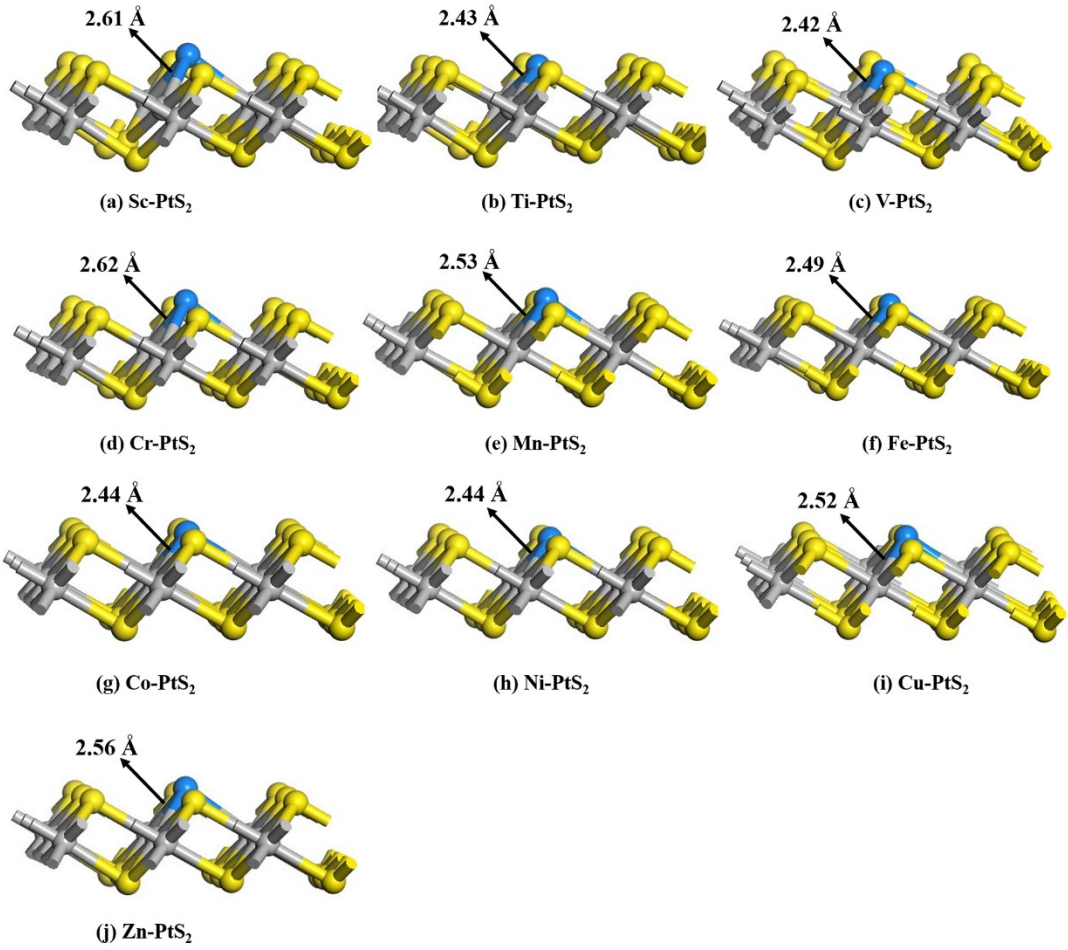

Fig. S1 Optimized structure of single TM atom anchored to the S-vacancy in 1T-PtS_2.

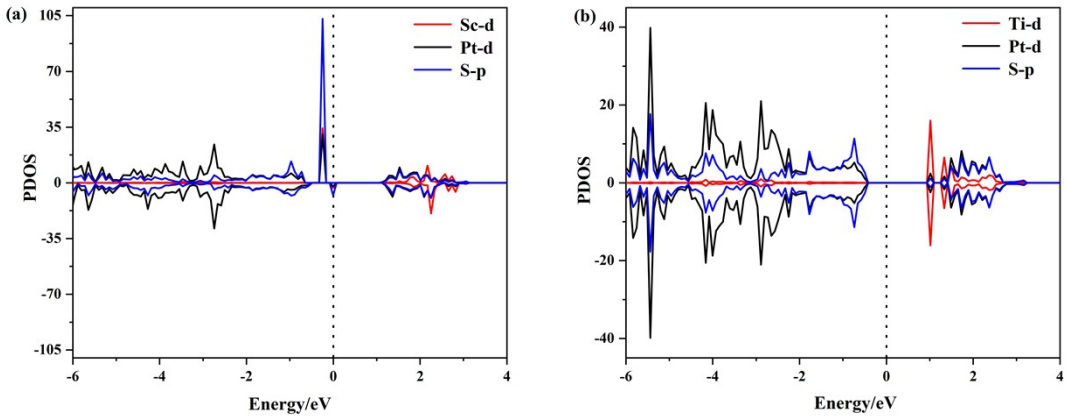

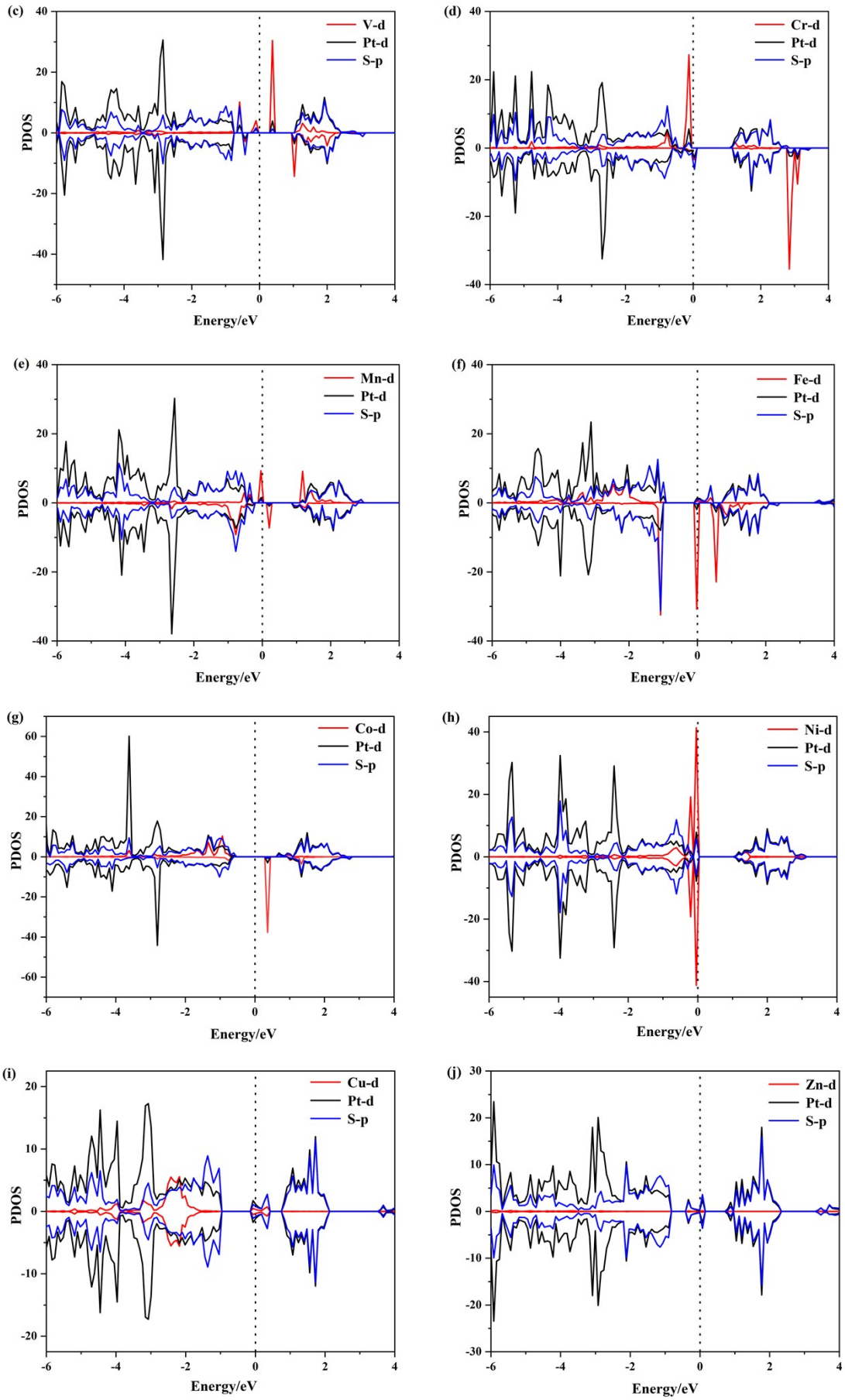
(c)
V-d
Pt-d
S-p
PDOS
Energy/eV
(d)
Cr-d
Pt-d
S-p
PDOS
Energy/eV
(e)
Mn-d
Pt-d
S-p
PDOS
Energy/eV
(f)
Fe-d
Pt-d
S-p
PDOS
Energy/eV
(g)
Co-d
Pt-d
S-p
PDOS
Energy/eV
(h)
Ni-d
Pt-d
S-p
PDOS
Energy/eV
(i)
Cu-d
Pt-d
S-p
PDOS
Energy/eV
(j)
Zn-d
Pt-d
S-p
PDOS
Energy/eV

Fig. S2 The partial density of states (PDOS) of TM-3d, Pt-5d and S-3p of TM-PtS_2

Table S1 Binding energies (E_b, eV) of the metal atom anchored on the S vacancy [E_b(TM-PtS_2)] and surface of PtS_2 [E_b (TM@PtS_2-Sv)], and the formation energies (E_f, eV) of the single TM atom and two TM atoms.

TM	E_b(TM-PtS_2)	E_b(TM@PtS_2-Sv)	E_f(TM-PtS_2)	E_f (TM_2-PtS_2)
Sc	-6.22	-5.32	-1.60	-
Ti	-6.69	-5.05	-0.53	0.66
V	-5.06	-3.69	0.87	1.19
Cr	-6.56	-2.53	0.87	1.26
Mn	-4.17	-1.17	-0.69	0.25
Fe	-4.46	-3.42	1.10	1.47
Co	-4.5	-3.34	1.08	1.48
Ni	-5.32	-3.96	0.31	0.98
Cu	-3.48	-2.46	0.38	1.78
Zn	-1.47	-0.43	-0.10	0.04

Table S2 Formation energy E_f (in eV) and dissolution potential U_{diss} of TM-PtS_2 (in V).

Catalysts	*Ef*	U^0_{diss} (metal)	*n*	U_{diss}
Sc-PtS_2	-1.6	-2.08	3	-1.55
Ti-PtS_2	-0.53	-1.63	2	-1.37
V-PtS_2	0.87	-1.18	2	-1.62
Cr-PtS_2	0.87	-0.91	2	-1.34
Mn-PtS_2	-0.69	-1.19	2	-0.85
Fe-PtS_2	1.10	-0.45	2	-1.00
Co-PtS_2	1.08	-0.28	2	-0.82
Ni-PtS_2	0.31	-0.26	2	-0.42
Cu-PtS_2	0.38	0.34	2	0.15
Zn-PtS_2	-0.1	-0.76	2	-0.71
Fe@1T'-MoS_2*	2.72	-0.45	2	-1.81
Co@1T'-MoS_2*	1.80	-0.28	2	-1.18
Ni@1T'-MoS_2*	1.62	-0.26	2	-1.07

* These are electrocatalysts that have been synthesized experimentally in Ref. 30.

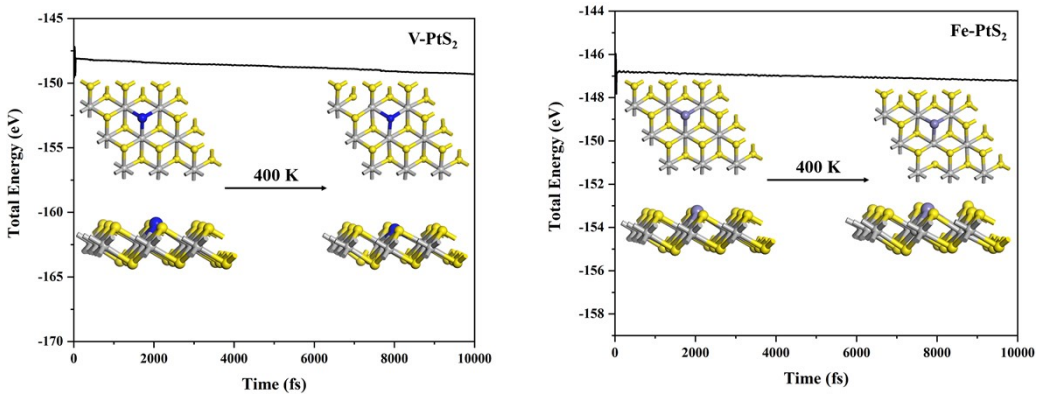

Fig. S4 Variations of energy as a function of the time for AIMD simulations with the solvation model on V- and Fe-PtS_2, and the insets show the corresponding geometry configurations for AIMD simulations at 0 ps and 10 ps

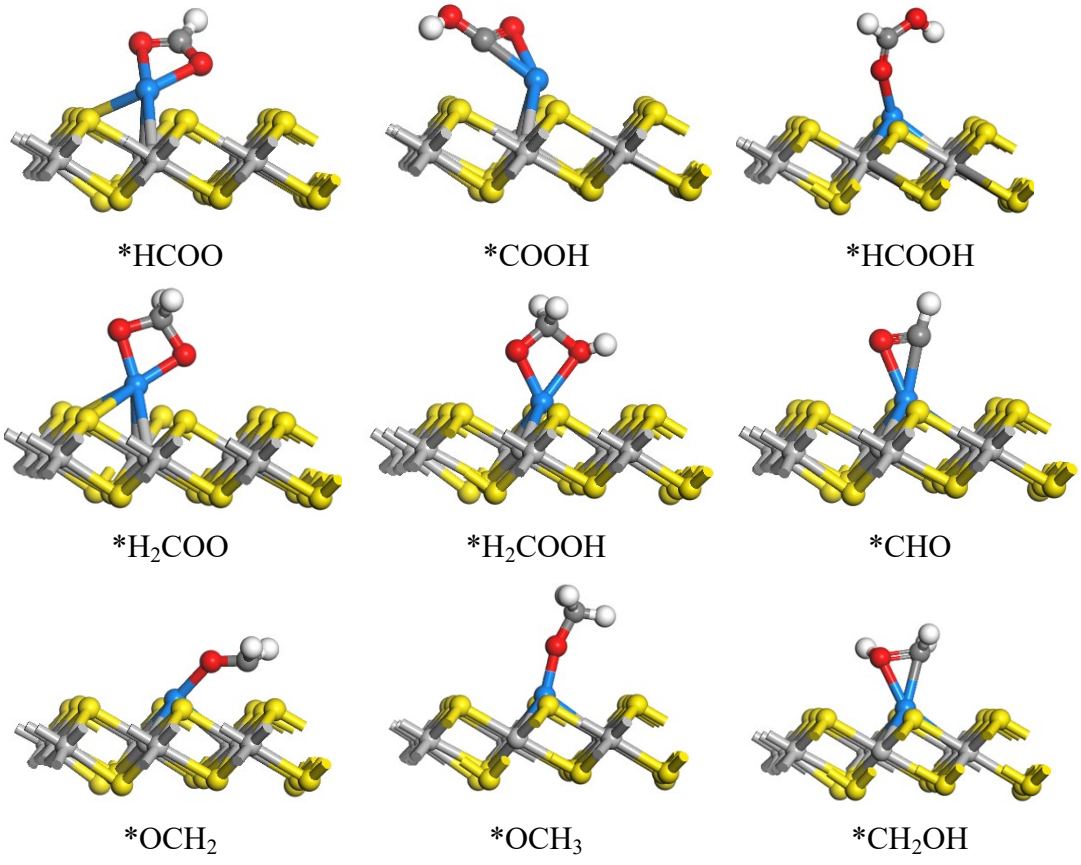

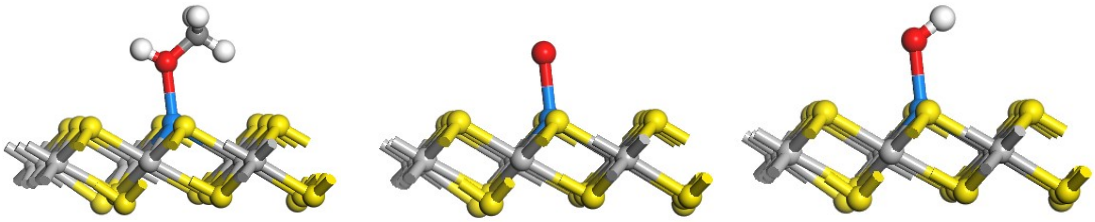

*CH_3OH *O *OH

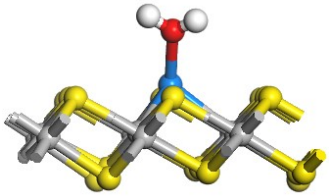

*H_2O

Fig. S5 Optimized structures of the CO_2RR involved intermediate species on Sc-PtS_2.

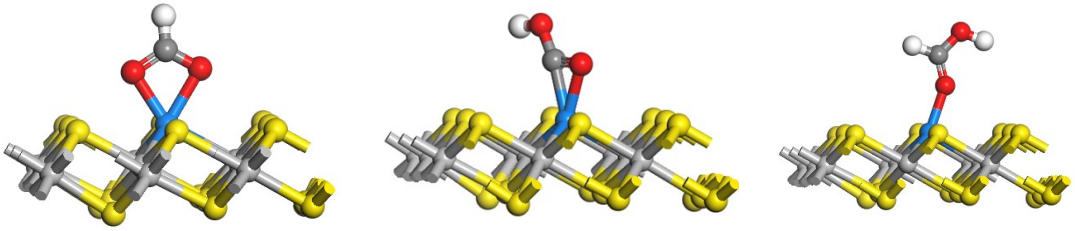

*HCOO *COOH *HCOOH

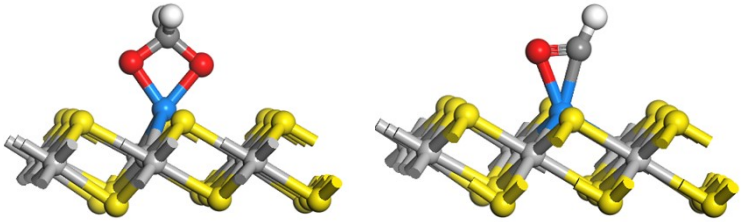

*H_2COO *HCO

Fig. S6 Optimized structures of the CO_2RR involved intermediate species on Ti-PtS_2.

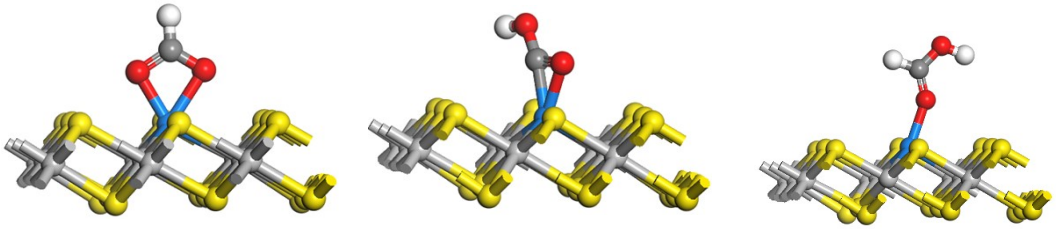

(a) *HCOO (b) *COOH (c) *HCOOH

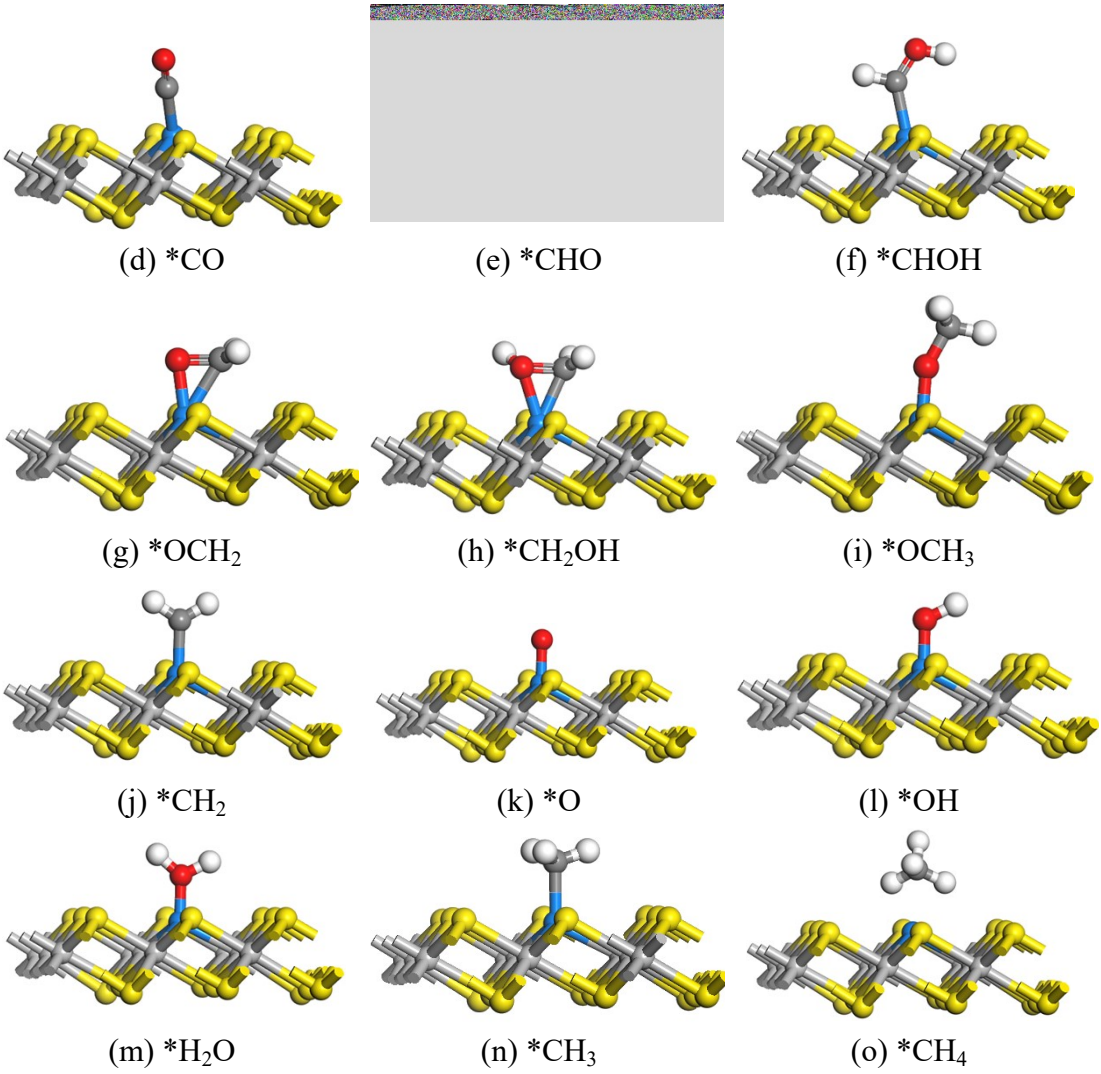

Fig. S7 Optimized structures of the CO_2RR involved intermediate species on V-PtS_2.

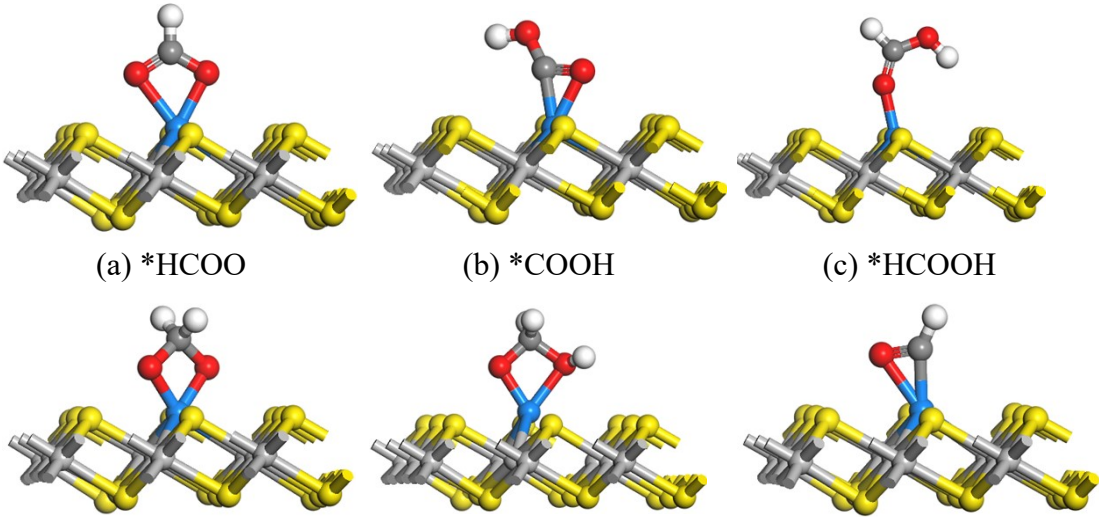

(d) *H_2COO (e) *H_2COOH (f) *CHO

Fig. S8 Optimized structures of the CO_2RR involved intermediate species on Cr-PtS_2.

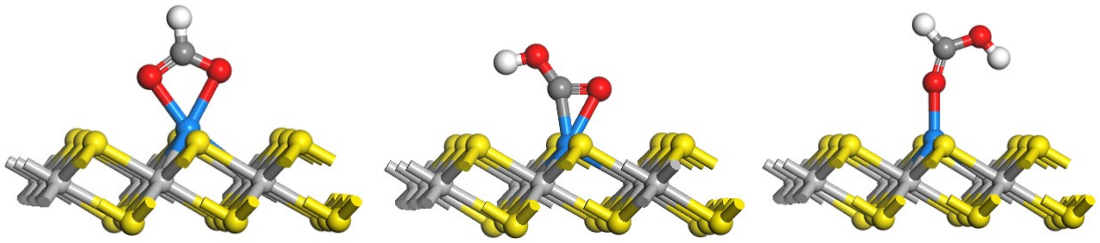

(a) *HCOO (b) *COOH (c) *HCOOH

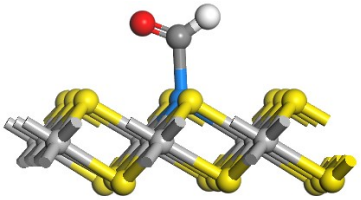

(d) *CHO

Fig. S9 Optimized structures of the CO_2RR involved intermediate species on Mn-PtS_2.

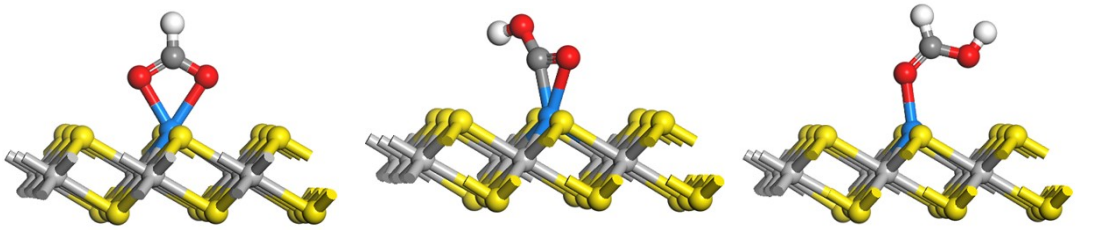

(a) *HCOO (b) *COOH (c) *HCOOH

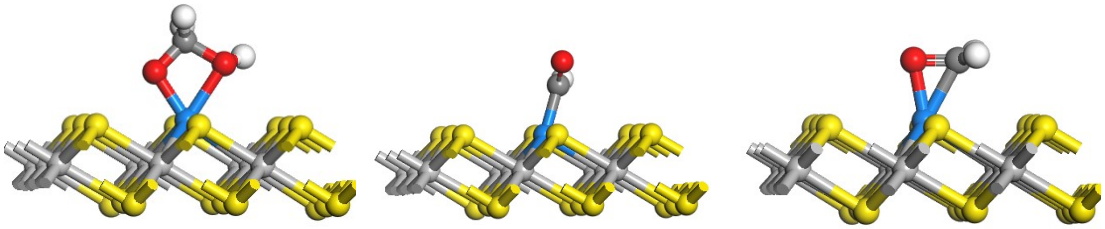

(d) *H_2COOH (e) *CHO (f) *OCH_2

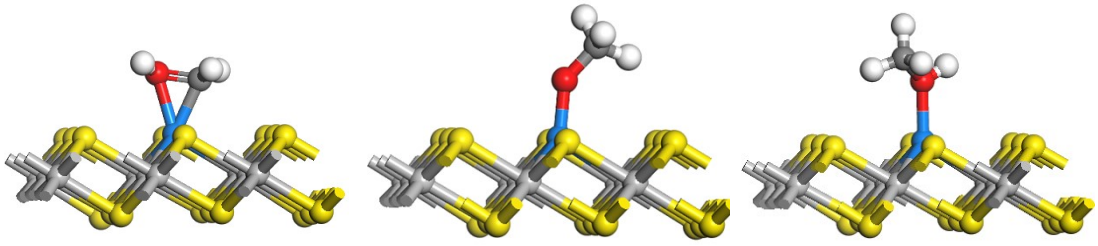

(g) *CH_2OH (h) *OCH_3 (i) *CH_3OH

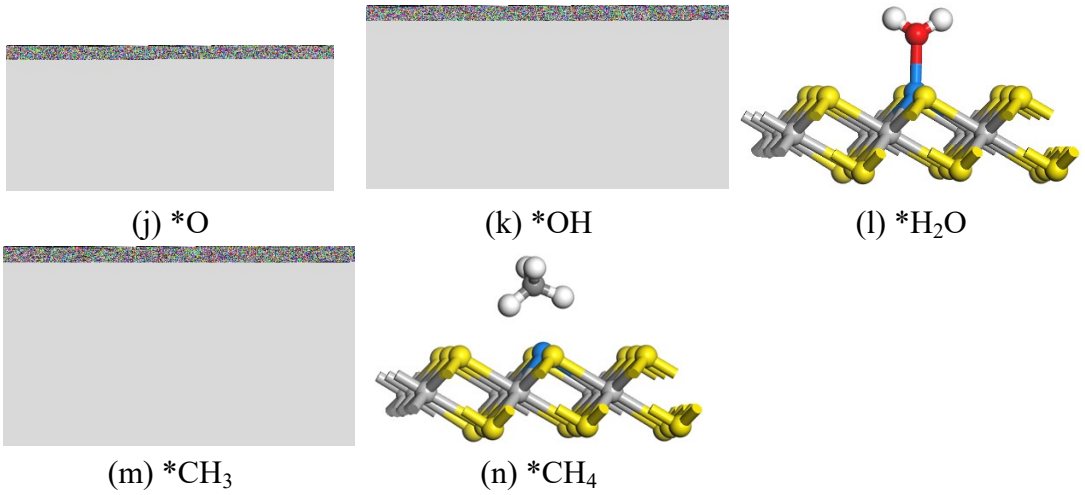

Fig. S10 Optimized structures of the CO_2RR involved intermediate species on Fe-PtS_2.

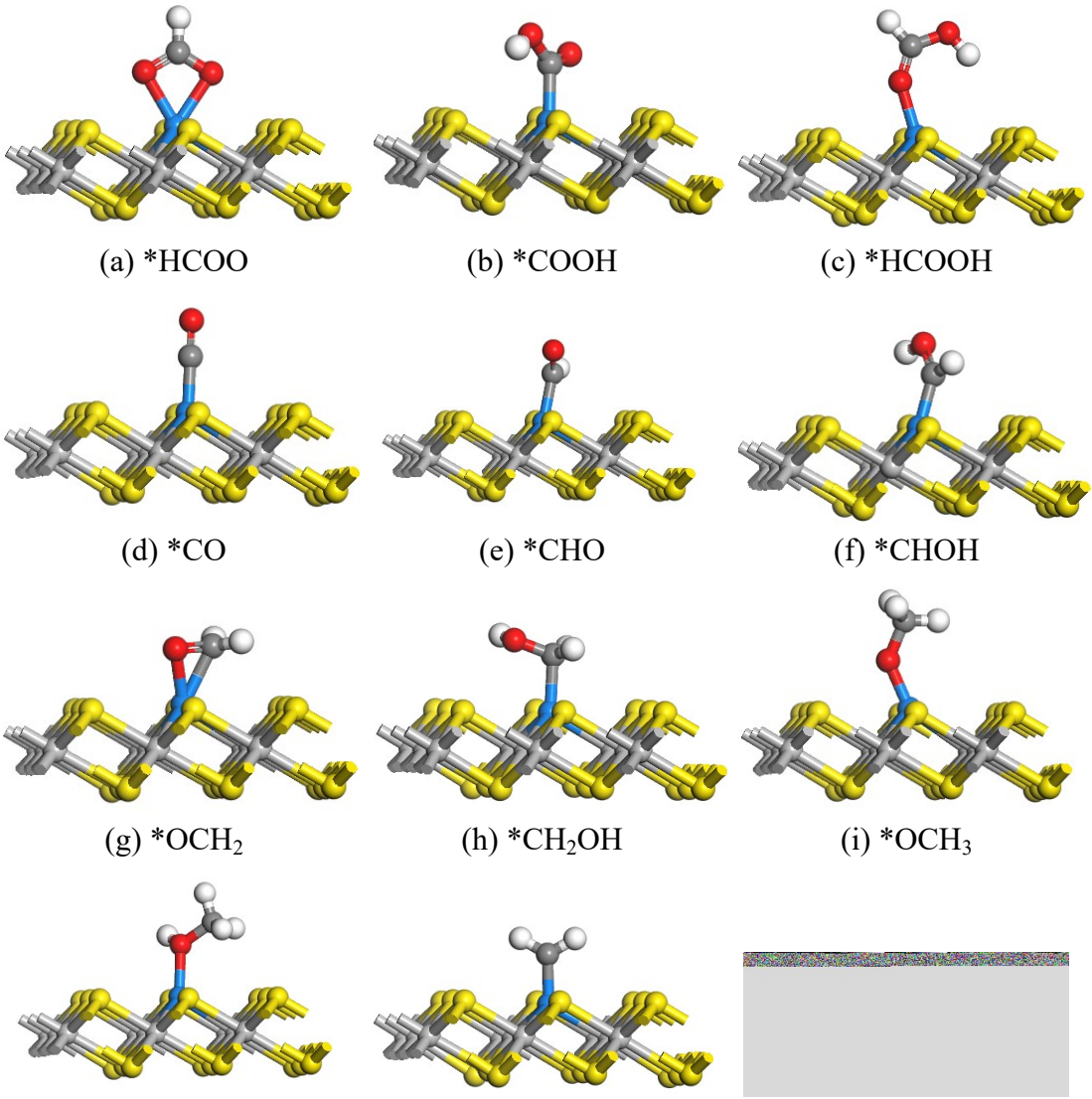

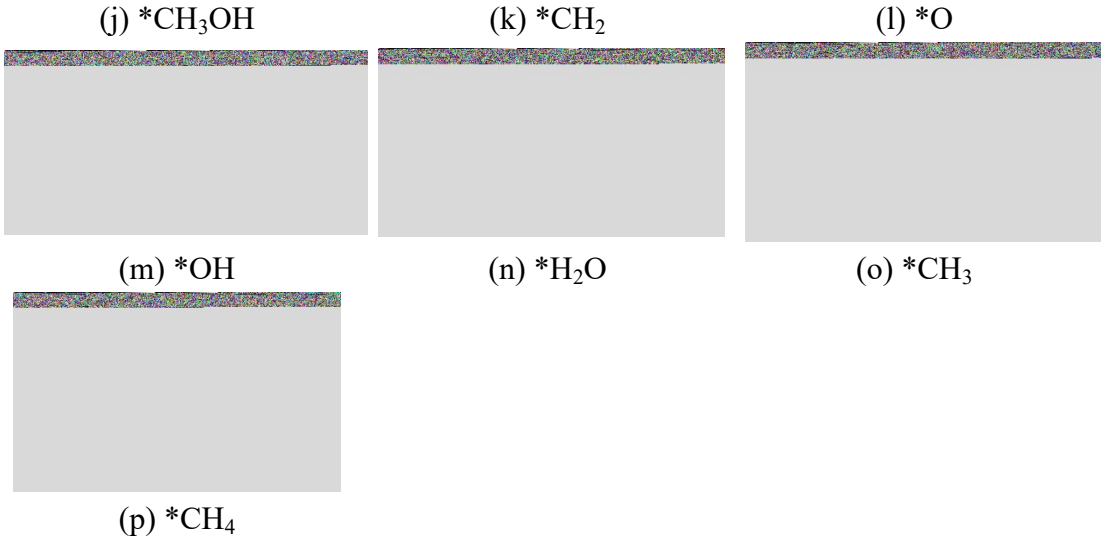

Fig. S11 Optimized structures of the CO_2RR involved intermediate species on Co-PtS_2.

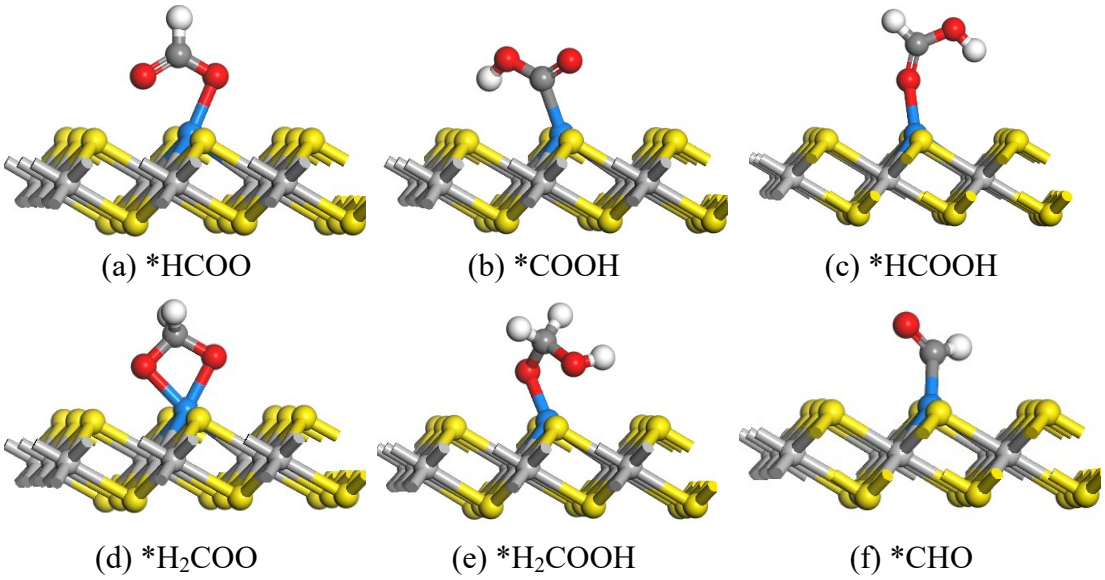

Fig. S12 Optimized structures of the CO_2RR involved intermediate species on Ni-PtS_2.

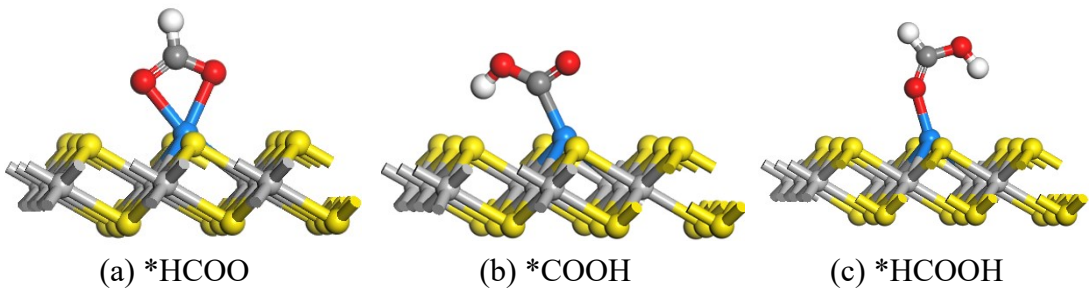

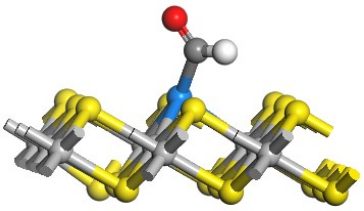

(d) *CHO

Fig. S13 Optimized structures of the CO_2RR involved intermediate species on Cu-PtS_2.

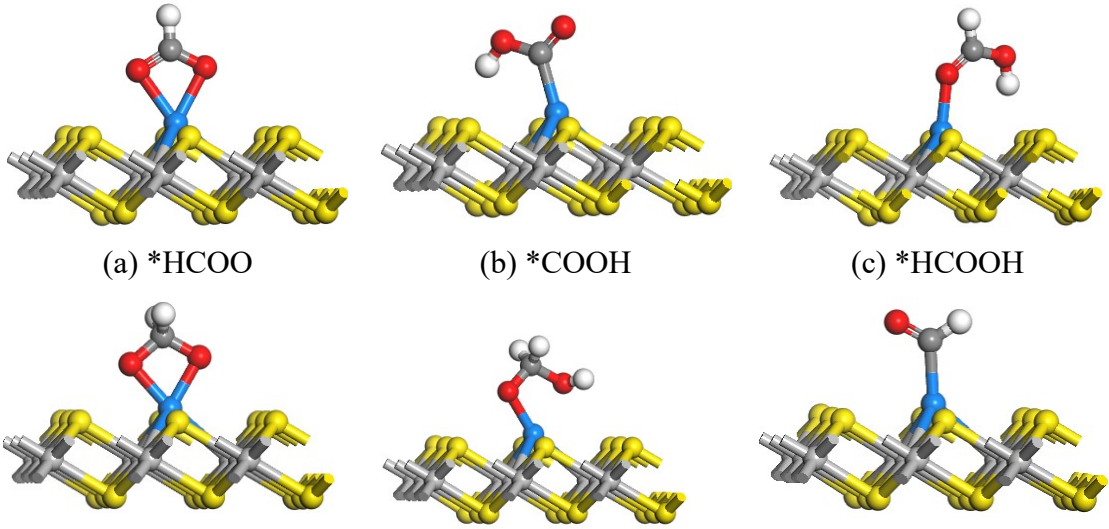

(a) *HCOO (b) *COOH (c) *HCOOH

(d) *H_2COO (e) *H_2COOH (f) *CHO

Fig. S14 Optimized structures of the CO_2RR involved intermediate species on Zn-PtS_2.

Table S3 Potential determining steps (PDS) of C_1 products and limiting potentials (U_L, V) of CO_2RR and HER on various TM-PtS_2 monolayers

catalyst	PDS	$U_L(CO_2RR)$	$U_L(HER)$	$U_L(HCOOH)$ -$U_L(H_2)$	Product
Sc	*+CO_2→*HCOO	-0.24	-2.26	2.02	HCOOH
	*+CO_2→*COOH	-1.39			CO
	HCOOH→H_2COOH	-0.86			CH_4/CH_3OH
Ti	*+CO_2→*HCOO	-0.41	-1.86	1.45	HCOOH
	*+CO_2→*COOH	-1.42			CO
	*HCOOH→*CHO	-1.46			CH_4/CH_3OH
V	*+CO_2→*COOH	-0.06	-0.63	0.57	HCOOH
	*COOH→*CO	-0.26			CO/CH_3OH
	OH→H_2O	-0.46			CH_4
Cr	*+CO_2→*HCOO	-0.39	-1.29	0.90	HCOOH
	*+CO_2→*COOH	-0.79			CO
	*HCOOH→*CHO	-1.15			CH_4
Mn	*+CO_2→*HCOO	-0.74	-1.35	0.61	HCOOH
	*+CO_2→*COOH	-2.10			CO
	*HCOOH→*CHO	-0.88			CH_4/CH_3OH
Fe	*HCOO→*HCOO	0	-0.70	0.70	HCOOH
	*+CO_2→*COOH	-0.64			CO
	HCOOH→H_2COOH	-0.32			*HCOOH→*H_2COOH

Co	*+CO_2→*HCOO	-0.23	-0.55	0.32	HCOOH/CH_4/CH_3OH
Ni	*+CO_2→*HCOO	-0.72	-0.95	0.23	HCOOH/CH_4/CH_3OH
Cu	*+CO_2→*HCOO	-0.25	-0.78	0.53	HCOOH
	*+CO_2→*COOH	-0.98			CO
	HCOOH→H_2COOH	-0.76			CH_4/CH_3OH
Zn	*HCOO→*HCOOH	-0.49	-0.53	0.04	HCOOH/CH_4/CH_3OH
	*+CO_2→*COOH	-1.02			